Direct observation of coupling between orientation and flow fluctuations in a nematic liquid crystal at equilibrium

Hiroshi Orihara,* Nobutaka Sakurai, and Yuji Sasaki
Division of Applied Physics, Hokkaido University, Sapporo 060-8628, Japan

Tomoyuki Nagaya
Department of Electrical and Electronic Engineering, Oita University, Oita 870-1192, Japan
(Received 11 January 2017; published 21 April 2017)

To demonstrate coupling between orientation and flow fluctuations in a nematic liquid crystal at equilibrium, we simultaneously observe the intensity change due to director fluctuations under a polarizing microscope and the Brownian motion of a fluorescent particle trapped weakly by optical tweezers. The calculated cross-correlation function of the particle position and the spatial gradient of the intensity is nonzero, clearly indicating the existence of coupling.

DOI: 10.1103/PhysRevE.95.042705

I. INTRODUCTION

Nematic liquid crystals (NLCs) have long-range orientational order, and the average direction of their rod-like molecules is designated by the so-called director. One of the most remarkable properties in NLCs is the coupling between director and flow: a change in the director can induce flow and vice versa. This coupling has been studied extensively from both fundamental and applied perspectives [1–9]. However, such investigations are typically confined to cases of large director changes and macroscopic flows, that is, nonequilibrium states. Although coupling should exist between director and flow fluctuations even at equilibrium, direct evidence is yet to be found; director and flow fluctuations at equilibrium are investigated separately at present. For example, changes in director are observed mainly by means of dynamic light scattering [10–13], and the results are fully explained by the Ericksen-Leslie (EL) theory [10,11]. Such changes can also be observed with a polarizing microscope [14,15]. This method allows us to observe long-wavelength modes of director fluctuation. In contrast, flow fluctuations are reflected in the Brownian motion of particles dispersed in a liquid crystal. The Brownian motion in liquid crystals is more complicated than usual isotropic liquids. For example, it was found that the local director distortion around a particle makes the Brownian motion anomalous: The mean-squared displacement (MSD) does not grow linearly with time [16].

In this paper, we demonstrate the existence of coupling between director and flow fluctuations at equilibrium by simultaneously observing the intensity changes due to director fluctuation under polarizers and the Brownian motion of a fluorescent particle trapped weakly by optical tweezers. In the next section, the basic idea for the demonstration and the experimental method are described. In Sec. III, experimental results are presented and discussed. Section IV is devoted to the conclusions.

II. EXPERIMENTAL METHOD

Here, we explain our basic idea for directly observing coupling between director and flow fluctuations. In general, thermal fluctuations at equilibrium can be decomposed into normal modes. As a simple case, we consider the coupling between a bend director mode and a shear flow mode, as shown in Fig. 1(a). The average direction of the director, $\vec{n}_0$, is in the y direction and the director tilts toward the x direction. On the other hand, the flow velocity is in the x direction. Both modes are changing sinusoidally in the y direction, that is, the wavenumber vectors are both in the y direction. We note that the phase difference between the tilt $\delta n_x(y)$ and the velocity $v_x(y)$ is $\pi/2$, as shown in Fig. 1(a). At point P, v_x becomes maximum and δn_x is zero, whereas the gradient $g_y^{(n)} \equiv \partial \delta n_x/\partial y$ in the y direction becomes minimum. Taking into account that the director motion should generate a flow, this indicates $v_x \propto \partial g_y^{(n)}/\partial t$, which will be derived later from the EL theory in Fourier space. Integration of this equation yields $x(t) - x(0) \propto g_y^{(n)}(t) - g_y^{(n)}(0)$. Here, x can be regarded as the position of a small particle put in the liquid crystal for flows with low Reynolds number. Therefore, the cross-correlation function $\langle (x(t) - x(0))(g_y^{(n)}(t) - g_y^{(n)}(0))\rangle$ becomes nonzero if there is a coupling between the orientation and the flow modes at equilibrium, through which we can demonstrate the existence of the coupling. Experimentally, it is easy to obtain $x(t)$, but not $g_y^{(n)}(t)$; $g_y^{(n)}(t)$ or $\delta n_x(t)$ can be related to the intensity of images under a polarizing microscope, as described later.

We used a planar cell with polyimide alignment layers. The gap was set to be 13 μm, which was determined according to a condition described later. The sample used was a low-birefringence nematic liquid crystal ZLI-2806 (Merck), which was required also to satisfy the above condition. By combining a polarizing microscope with a band-pass filter of 550 nm and a fluorescent microscope, we simultaneously observed the transmitted intensity change due to the director fluctuations and the Brownian motion of a fluorescence polystyrene particle with a diameter of 1 μm (Fluospheres, Invitrogen) dispersed in the liquid crystal. The particle was weakly trapped with optical tweezers (1064 nm, 10 mW) and observations were made at three different heights. We captured 8192 images with a size of

*orihara@eng.hokudai.ac.jp

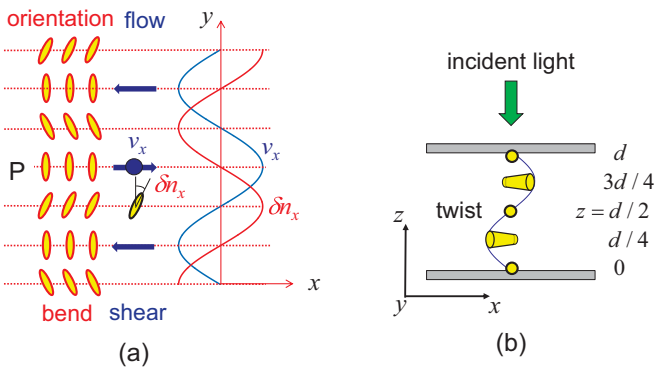

FIG. 1. (a) Coupling between bend deformation of δn_x and shear flow of v_x, which both fluctuate sinusoidally with a wave number along the y axis. At the point P, v_x becomes maximum, whereas the spatial gradient of δn_x becomes minimum. (b) Twist deformation along the z axis. The amplitude of the bend deformation in the $x-y$ plane depends on z: it is maximum at $z = d/4$ and $3d/4$, whereas it vanishes at $z = d/2$. It should be noted that the phases at $z = d/4$ and $3d/4$ are opposite, indicating that the corresponding flow velocities are also opposite.

512×512 pixels ($52 \times 52\,\mu\text{m}^2$) and a frame rate of 100 fps for each run, and made a total of 15 runs. The temperature was kept at 25°C during the measurements.

A typical image is shown in Fig. 2. The particle is trapped at the center by the optical tweezers, but the Brownian motion can be observed. The spatial change in intensity is due to the director fluctuations, and the temporal change can be seen in a video in the Supplemental Material [17]. The observed intensity fluctuation $\delta I(x,y)$ is derived approximately in the Appendix:

$$\delta I(x,y) = c\frac{2}{d}\text{Im}\left[\int_0^d \delta n_x(x,y,z')\exp(i\Delta q z')dz',\right], \quad (1)$$

where c is a constant having the same dimension with $\delta I(x,y)$, $\delta n_x(x,y,z)$ is the director fluctuation, d is the cell gap, and

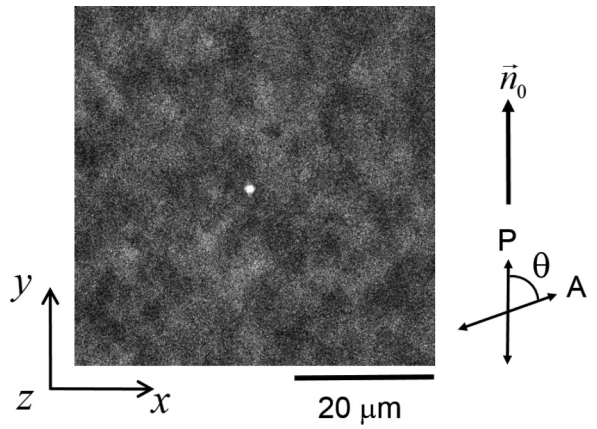

FIG. 2. Typical image obtained by combining a polarizing microscope and a fluorescence microscope. The angle between the polarizer and analyzer, θ, is set to be 72°. The spatial fluctuations of δn_x are represented by the intensity changes, and the temporal change can be seen in a video [17]. A particle is trapped at the center.

$\Delta q = 2\pi/\lambda \cdot \Delta n$; in this, the wavelength of light in vacuum is λ, and the refractive index anisotropy is Δn. The director fluctuation $\delta n_x(x,y,z)$ can be expanded in a Fourier series as

$$\delta n_x(x,y,z) = \sum_{\vec{q}} \delta n_x(q_x,q_y,q_z)\exp[i(q_x x + q_y y)]\sin q_z z, \quad (2)$$

where $q_z = m\pi/d (m = 1,2,\ldots)$, from the boundary condition of $\delta n_x(x,y,z) = 0$ at $z = 0$ and d. If we choose $d = 2\pi/\Delta q = \lambda/\Delta n$, we can obtain a simple relation from Eqs. (1) and (2):

$$\delta I(q_x,q_y) = c\delta n_x(q_x,q_y,\Delta q), \quad (3)$$

where $\delta I(q_x,q_y)$ is the Fourier coefficient of $\delta I(x,y)$. Using q_x, q_y, and Δq, the condition for the approximation used in deriving Eq. (1) to be valid is $q_x, q_y \ll \Delta q$. This condition indicates that the mode related to $\delta n_x(q_x,q_y,\Delta q)$ should be the so-called mode 2 [10], in which the fluctuation $\delta\vec{n}$ is perpendicular to the plane spanned by $\vec{n}_0$ and $\vec{q}$. Equation (3) means that we can observe director modes with $q_z = \Delta q = 2\pi/d$, that is, with just one wave in the z direction, as shown in Fig. 1(b). As seen from Figs. 1(a) and 1(b), the observable modes are a mixture of bend and twist deformations: there is a bend deformation along the y direction and a twist deformation along the z direction. For our low-birefringence liquid crystal ZLI-2806 with $\Delta n = 0.0437$, we have $d(= \lambda/\Delta n) \cong 13\mu$m for the light wavelength of 550 nm used in the measurements. For a typical liquid crystal 5CB, in contrast, $d \cong 3\mu$m, which is too small for our measurements, in which we use a 1-μm particle. This is the reason we chose ZLI-2806. The constant c will be determined in the next section.

III. EXPERIMENTAL RESULTS AND DISCUSSIONS

When we perform the Fourier transformation to obtain $\delta I(q_x,q_y)$, we mask the particle to avoid the effect of its motion. In Fig. 3(a), we show the time correlation function $\langle|\delta I(q_x,q_y,t) - \delta I(q_x,q_y,0)|^2\rangle$ at $q_x = 0$ and several values of q_y. From the EL theory, the correlation function is given as $2\langle|\delta I(q_x,q_y)|^2\rangle(1 - \exp[-t/\tau(q_x,q_y)])$, where $\tau(q_x,q_y)$ is the relaxation time, which depends on the viscosity coefficients and so on [10]. Figure 3(b) shows the inverse of $\langle|\delta I(q_x,q_y)|^2\rangle$, obtained from Fig. 3(a) by least-squares fitting, as a function of q_x^2 at $q_y = 0$ and as a function of q_y^2 at $q_x = 0$. From the equipartition theorem and Eq. (3), the inverse of the mean-squared intensity fluctuation for mode 2 is given by

$$\begin{aligned}\langle|\delta I(q_x,q_y)|^2\rangle^{-1} &= c^{-2}\langle|\delta n_x(q_x,q_y)|^2\rangle^{-1} \\ &= (c^2 k_B T)^{-1} V\left\{K_2\left(q_x^2 + \Delta q^2\right) + K_3 q_y^2\right\},\end{aligned} \quad (4)$$

where k_B is the Boltzmann constant, V is the volume of the observed region, and K_2 and K_3 are the twist and bend elastic constants, respectively. From the slopes and the intersection with the vertical axis in Fig. 3(b), the constant c was determined using Eq. (4). The averaged value of c is 0.30×10^4, where we used $V = 3.6 \times 10^{-14}\,\text{m}^3$, $K_2 = 7.9\,\text{pN}$, and $K_3 = 15.4\,\text{pN}$ [18].

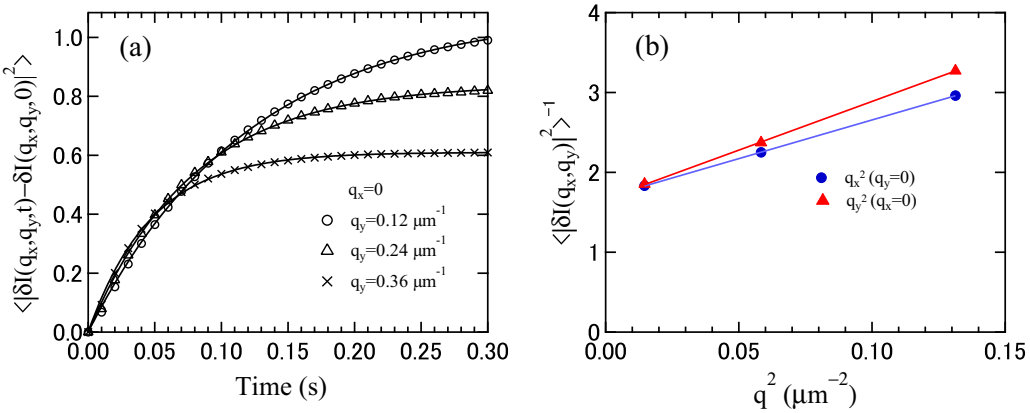

FIG. 3. (a) Time correlation functions of image intensity at $q_x = 0$ and several values of q_y. (b) Inverse of $\langle|\delta I(q_x,q_y)|^2\rangle$, obtained from Fig. 3(a) by least-squares fitting, as a function of q_x^2 at $q_y = 0$ and as a function of q_y^2 at $q_x = 0$.

Next, we show the mean-squared displacements (MSDs) of the particle along the x and y directions at a height of $z = d/4$. After tuning the brightness and the contrast of the image in Fig. 2, we obtained the position of the particle and calculated its MSDs. As shown in Fig. 4, the MSD in the y or $\vec{n}_0$ direction is larger than that in the x direction because of the anisotropy of diffusion [16]. Although both MSDs are slightly curved, mainly because of the optical trap, we ignore this effect in the following theoretical analyses.

Before presenting the experimentally obtained cross-correlation function, we derive it theoretically based on EL theory. For mode 2, the equations of motion for $\delta n_x(\vec{q})$ and $v_x(\vec{q})$ [defined in the same way as $\delta n_x(\vec{q})$ using Eq. (2)] are [10,11]

$$\gamma_1 \frac{\partial \delta n_x(\vec{q})}{\partial t} = -K_2(\vec{q})\delta n_x(\vec{q}) - iC_2(\vec{q})v_x(\vec{q}), \tag{5a}$$

$$\rho \frac{\partial v_x(\vec{q})}{\partial t} = iQ_2(\vec{q})\frac{\partial \delta n_x(\vec{q})}{\partial t} - P_2(\vec{q})v_x(\vec{q}), \tag{5b}$$

where $K_2(\vec{q})$ is a function of the wave number and the Frank elastic constants; $C_2(\vec{q})$, $Q_2(\vec{q})$, and $P_2(\vec{q})$ are functions of the wave number and the Leslie viscosity coefficients; γ_1 is the rotational viscosity coefficient; and ρ is the mass density.

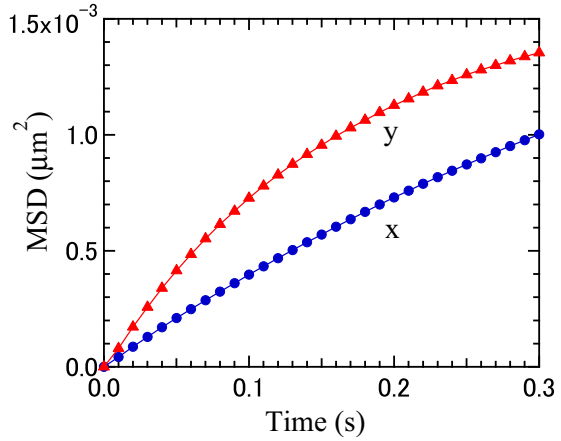

FIG. 4. Mean-squared displacements (MSDs) obtained from Fig. 2 in the x and y directions.

In our case, we can neglect the inertia term in Eq. (5b) so that we obtain

$$v_x(\vec{q}) = if(\vec{q})\frac{\partial \delta n_x(\vec{q})}{\partial t} \tag{6a}$$

with

$$f(\vec{q}) = Q_2(\vec{q})/P_2(\vec{q}) = \frac{2\alpha_2 q_y}{\alpha_4\left(q_x^2 + \Delta q^2\right) + (-\alpha_2 + \alpha_4 + \alpha_5)q_y^2}, \tag{6b}$$

where α_i are the Leslie viscosity coefficients. Equation (6a) corresponds to $v_x \propto \partial g_y/\partial t$, as shown before. Substituting Eq. (6a) into Eq. (5a) yields a closed equation of motion for $\delta n_x(\vec{q})$, which has the same form as Eq. (5a) except that γ_1 is replaced by $\gamma_1 - f(\vec{q})C_2(\vec{q})$. This means that the viscosity should depend on $\vec{q}$ when the coupling with the flow is considered. This has in fact been observed in light-scattering experiments [13], although this is indirect evidence of coupling. We directly verify Eq. (6a) itself.

Assuming that the particle is trapped near $\vec{r} = (0,0,z_p)$, its displacement during the time interval t can be rewritten using Eq. (6a):

$$\begin{aligned} x(t) - x(0) &= \int_0^t v_x(x(\tau),y(\tau),z(\tau),\tau)d\tau \\ &\cong \int_0^t v_x(0,0,z_p,\tau)d\tau \\ &= \int_0^t \sum_{\vec{q}} v_x(\vec{q},\tau)\sin q_z z_p d\tau \\ &= \int_0^t \sum_{\vec{q}} if(\vec{q})\frac{\partial \delta n_x(\vec{q},\tau)}{\partial \tau}\sin q_z z_p d\tau \\ &= \sum_{\vec{q}} if(\vec{q})\sin q_z z_p(\delta n_x(\vec{q},t) - \delta n_x(\vec{q},0)), \end{aligned} \tag{7}$$

where we have replaced $v_x(x(\tau),y(\tau),z(\tau),\tau)$ by $v_x(0,0,z_p,\tau)$ because here we consider only long-wavelength modes.

Equation (7) relates the particle displacement to the director reorientation. Next, we need the gradient $g_y^{(n)} = \partial \delta n_x / \partial y$, which was defined when we explained our basic idea. However, instead we shall use $g_y \equiv c^{-1} \partial \delta I / \partial y$ because the observable is $\delta I(x,y)$ in our experiments, and the constant c is introduced to make a nondimensional $c^{-1} I$. It is difficult to obtain g_y directly at the particle position because we cannot correctly observe the intensity change due to the director fluctuations near the particle, which is seriously affected by the fluorescent light emitted by the particle. Therefore, we use the Fourier coefficients of $\delta I(x,y)$, in terms of which g_y is expressed as

$$g_y = c^{-1} \frac{\partial \delta I}{\partial y}\bigg|_{x=y=0} = c^{-1} \sum_{q_x,q_y} i q_y \delta I(q_x,q_y) = \sum_{q_x,q_y} i q_y \delta n_x(q_x,q_y,\Delta q), \tag{8}$$

where we have used Eq. (3). Thus, we can calculate the cross-correlation function from Eqs. (7) and (8):

$$\langle (x(t)-x(0))(g_y(t)-g_y(0)) \rangle = \sin \Delta q z_p \sum_{q_x,q_y} q_y f(q_x,q_y,\Delta q) \langle |\delta n_x(q_y,q_y,\Delta q,t) - \delta n_x(q_y,q_y,\Delta q,0)|^2 \rangle, \tag{9}$$

where we have used the property that each mode is independent, expressed as $\langle \delta n_x(\vec{q}_1,t_1)^* \delta n_x(\vec{q}_2,t_2) \rangle = \delta_{\vec{q}_1,\vec{q}_2} \langle \delta n_x(\vec{q}_1,t_1)^* \delta n_x(\vec{q}_1,t_2) \rangle$. It is clear from Eq. (9) that, in general, if the coupling coefficient $f(\vec{q})$ is nonzero (i.e., there is coupling between the orientation and the flow), then we can observe a nonzero cross-correlation function and vice versa. Here, we note that Eq. (9) has a factor $\sin \Delta q z_p$ that depends on the height of the particle. Since $\Delta q = 2\pi/d$ in our case, this factor takes values of, for example, -1 at $z_p = 3d/4$, 0 at $z_p = d/2$, and $+1$ at $z_p = d/4$.

In Eq. (8), we are not allowed to sum overall q_x and q_y because of the condition $q_x, q_y \ll \Delta q$; instead, we include only small q_x and q_y in the summation: $q_x = 2\pi m_x/L$ and $q_y = 2\pi m_y/L$, where m_x and m_y are integers satisfying $-3 \leqslant m_x, m_y \leqslant 3$, and $L(=52\mu\text{m})$ is the size of the observed area. The cross-correlation functions at the three heights $z_p = 3d/4$, $d/2$, and $d/4$ obtained from the approximated g_y are shown in Fig. 5. The cross-correlation functions at $z_p = 3d/4$ and $z_p = d/4$ are nonzero and have opposite signs, whereas the one at $z_p = d/2$ is almost zero, as is predicted from Eq. (9). The initial increase or decrease is also explained by Eq. (9), in which the time dependence of the cross-correlation function is fully determined by the auto-correlation functions of the director fluctuations in our case, in which the inertia is treated as negligible.

Last, we show the validity of Eq. (9) by calculating its right-hand side from the experimentally obtained autocorrelation functions. To do so, we need to numerically calculate $f(\vec{q})$, given in Eq. (6b), but there are no available data on the Leslie viscosity coefficients. Fortunately, however, $f(\vec{q})$ depends on only the ratios of the viscosities, so we simply assume $\alpha_2 : \alpha_4 : \alpha_5 = -1 : 1 : 1$. This may be allowed because, for typical liquid crystals, $\alpha_2 : \alpha_4 : \alpha_5 = -1 : 1.1 : 0.7$ for MBBA [19] and $\alpha_2 : \alpha_4 : \alpha_5 = -1 : 0.8 : 0.8$ for 5CB [20]. The calculated

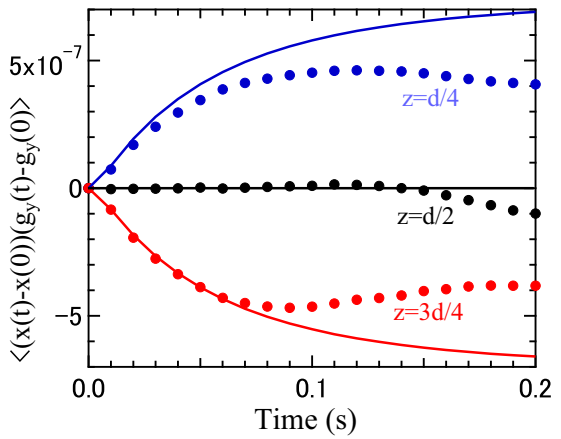

FIG. 5. Cross-correlation functions $\langle (x(t)-x(0))(g_y(t)-g_y(0)) \rangle$ obtained at $z = d/4, d/2$, and $3d/4$. Solid lines are calculated from Eq. (9).

cross-correlation functions are also shown in Fig. 5, where the sum in Eq. (9) is taken over the same q_x and q_y used in Eq. (8). We obtain satisfactory agreement despite some rough approximations having been made. The discrepancy in the long-time regime may be due to the optical trap.

Here, it should be noted that the above results are valid even if we consider the director distortion around the particle, which gives rise to the anomalous Brownian motion, as mentioned in the introduction. The characteristic size of the distortion may be equal to the cell thickness. In our analysis, however, we used director fluctuations with wavelengths longer than it. Therefore, the gradient g_y in Eq. (8) doesn't include the information on the director distortion around the particle so that the information should disappear in the cross-correlation function though x has it. However, we would like to mention that the direct coupling of the particle movement with the director fluctuations through the anchoring on the particle surface may be observed with another analyses.

IV. CONCLUDING REMARKS

We have successfully demonstrated the existence of coupling between director orientation and flow fluctuations at equilibrium by obtaining a nonzero cross-correlation function of the spatial gradient of the intensity and the particle position. The cross-correlation function was shown to depend on the particle height, which was explained by the dependence of the flow direction on the same quantity. These results were fully understood in the context of EL theory.

In closing, we would like to point out that the coupling might modify the Brownian motion of a particle in a NLC. From Eq. (7), we can easily obtain

$$\langle (x(t)-x(0))^2 \rangle = \sum_{\vec{q}} (f(\vec{q}) \sin q_z z_p)^2 \langle |\delta n_x(\vec{q},t) - \delta n_x(\vec{q},0)|^2 \rangle. \tag{10}$$

We note that the actual MSD is the sum of Eq. (10) and the intrinsic MSD irrelevant to the coupling. The right-hand side of Eq. (10) increases monotonically as a function of time and becomes constant in the long-time regime, indicating

that the actual MSD cannot follow the typical diffusion of MSD $\propto t$. In the present experiments, we were unable to detect the anomalous diffusion because of the optical trap, which made the MSD constant in the long-time regime. We intend to clarify the effect of the director fluctuations on the Brownian motion in future work.

ACKNOWLEDGMENTS

This work was supported by JSPS KAKENHI Grants No. JP25103006 and No. JP26289032.

APPENDIX

Here, we derive Eq. (1). In our experiments, as shown in Fig. 1(b), polarized light along the y axis is incident along the $-z$ axis (i.e., downward). We solve the Maxwell equations

$$\mathrm{rot}\vec{H} = \varepsilon_0 \varepsilon \frac{\partial \vec{E}}{\partial t}, \tag{A1}$$

$$\mathrm{rot}\vec{E} = -\mu_0 \frac{\partial \vec{H}}{\partial t}, \tag{A2}$$

where ε_0 and μ_0 are the dielectric and magnetic permittivities, respectively, of a vacuum, and ε is the relative dielectric permittivity. For nematic liquid crystals, ε is a function of $\vec{n}$:

$$\varepsilon_{\alpha\beta} = \varepsilon_\perp \delta_{\alpha\beta} + \Delta\varepsilon n_\alpha n_\beta, \tag{A3}$$

where $\Delta\varepsilon = \varepsilon_\parallel - \varepsilon_\perp$ with $\varepsilon_\parallel$ and $\varepsilon_\perp$ being the relative dielectric permittivities parallel and perpendicular, respectively, to the director.

First, we assume that the director depends only on the z coordinate (i.e., $\vec{n}(z)$) and expresses the incident light as

$$E_y(z,t) = E_0 \exp(-iq_\parallel z)\exp(-i\omega t), \tag{A4}$$

with

$$q_\parallel = \omega/c \cdot \sqrt{\varepsilon_\parallel}, \tag{A5}$$

where c is the speed of light in a vacuum. The incident light is scattered by the fluctuation $\delta n_x(z)$, generating the x component of the electric field, $E_x(z,t) = \delta E_x(z)\exp(-i\omega t)$. By using the perturbation method with respect to $\delta n_x(z)$, we obtain $\delta E_x(z)$ from Eqs. (A1)–(A3):

$$\frac{\partial^2 \delta E_x}{\partial z^2} = -q_\perp^2 \delta E_x - q_0^2 \Delta\varepsilon \delta n_x E_0 \exp(-iq_\parallel z), \tag{A6}$$

where $q_\perp = \omega/c \cdot \sqrt{\varepsilon_\perp}$ and $q_0 = \omega/c$. If reflections at the interfaces between the liquid crystal and the glass plates are negligible, the above equation can be solved as

$$\delta E_x(z) = i\frac{q_0^2}{2q_\perp}\Delta\varepsilon E_0 \left\{ \exp(-iq_\perp z)\int_z^d \delta n_x(z')\exp[-i(q_\parallel - q_\perp)z']dz' + \exp(iq_\perp z)\int_0^z \delta n_x(z')\exp[-i(q_\parallel + q_\perp)z']dz' \right\} \quad (0 \leqslant z \leqslant d). \tag{A7}$$

We can put an analyzer at $z = 0$ without loss of generality. In this case, the electric field just after passing the analyzer shown in Fig. 2 is given as

$$E_A = E_0 \cos\theta + \delta E_x(0)\sin\theta. \tag{A8}$$

Thus, the intensity related to the director fluctuation is obtained from $|E_A|^2$ by using Eq. (A7):

$$2\mathrm{Re}[E_0 \delta E_x(0)]\sin\theta\cos\theta = c'\frac{2}{d}\mathrm{Im}\left[\int_0^d \delta n_x(z')\exp(i\Delta q z')dz'\right], \tag{A9}$$

with

$$c' = \frac{q_0^2 d}{4q_\perp}\Delta\varepsilon E_0^2 \sin 2\theta. \tag{A10}$$

When the spatial change of the director in the x and y directions is smaller than that in the z direction (i.e., for the case that the wavenumber along the x and y directions is smaller than that along the z direction), we can replace $\delta n_x(z')$ by $\delta n_x(x,y,z')$ in Eq. (A9), resulting in Eq. (1).

[1] D. W. Berreman, J. Appl. Phys. **46**, 3746 (1975).
[2] P. E. Cladis and S. Torza, Phys. Rev. Lett. **35**, 1283 (1975).
[3] H. Stark and D. Ventzki, Phys. Rev. E **64**, 031711 (2001).
[4] C. Denniston, E. Orlandini, and J. M. Yeomans, Phys. Rev. E **63**, 056702 (2001).
[5] G. Tóth, C. Denniston, and J. M. Yeomans, Phys. Rev. Lett. **88**, 105504 (2002).
[6] C. Blanc, D. Svensek, S. Zumer, and M. Nobili, Phys. Rev. Lett. **95**, 097802 (2005).
[7] S. A. Jewell and J. R. Sambles, Phys. Rev. E **73**, 011706 (2006).
[8] O. P. Pishnyak, S. Tang, J. R. Kelly, S. V. Shiyanovskii, and O. D. Lavrentovich, Phys. Rev. Lett. **99**, 127802 (2007).
[9] Y. Zhou, T. Tsuji, and S. Chono, Appl. Phys. Lett. **109**, 011902 (2016).

[10] P. G. de Gennes and J. Prost, *The Physics of Liquid Crystals*, 2nd ed., International Series of Monographs on Physics (Oxford Science Publications, Oxford, UK, 1993), Chaps. 3.4 and 5.2.5.

[11] S. Chandrasekhar, *Liquid Crystals*, 2nd ed. (Cambridge University Press, Cambridge, 1992), Chap. 3.9.

[12] W. H. de Jeu, *Physical Properties of Liquid Crystalline Materials* (Gordon & Breach, New York, 1980).

[13] Orsay Liquid Crystal Group, J. Chem. Phys. **51**, 816 (1969).

[14] H. Orihara, Y. Sato, T. Nagaya, and Y. Ishibashi, J. Phys. Soc. Jpn. **67**, 2565 (1998).

[15] H. Orihara, A. Sakai, and T. Nagaya, Mol. Cryst. Liq. Cryst. **366**, 143 (2001).

[16] T. Turiv, I. Lazo, A. Brodin, B. I. Lev, V. Reiffenrath, V. G. Nazarenko, and O. D. Lavrentovich, Science **342**, 1351 (2013).

[17] See Supplemental Material at http://link.aps.org/supplemental/10.1103/PhysRevE.95.042705. The movie is played at a rate twice slower than real.

[18] R. P. Trivedi, D. Engstrom, and I. I. Smalyukh, J. Opt. **13**, 044001 (2011).

[19] C. Gauhwiller, Mol. Cryst. Liq. Cryst. **20**, 301 (1973).

[20] G. Ahlers, in *Pattern Formation in Liquid Crystals*, edited by L. Kramer and A. Buka (Springer, Berlin, 1996).